Ionization differences between weak and strong electrolytes: the role of protonic quantum effects as perturbed by dielectric relaxation spectroscopy

Vasily G. Artemov,* Alexander Ryzhov, Henni Ouerdane, and Keith Stevenson

Center for Energy Science and Technology, Skolkovo Institute of Science and Technology, 121205 Moscow, Russia

E-mail: v.artemov@skoltech.ru

Abstract

Revealing the microscopic dynamics, including protonic quantum effects, in aqueous electrolyte solutions has been a challenge for modern experimental methods and molecular dynamics simulations of the past decade. These properties are out of the scope of the standard electrolytic dissociation model and leave a gap between theory and experiment due to the lack of details of the fast molecular dynamics during solvation. We report a dielectric-spectroscopy study (1Hz to 20 GHz), which unambiguously demonstrates a net difference in the dynamic structures of weak and strong electrolytes, shedding new light on the mechanism of solvation via proton exchange reactions. Based on these data, we suggest an extension of Arrhenius' seminal model, providing a more accurate description of the electrical properties of electrolytes over a wide range of concentrations (10^{-7} to 10 M). We show that dissolved species of weak electrolytes more likely interact with each other than with the solvent, preventing dissociation and explaining a sharp difference between weak and strong electrolytes. These results extend our understanding of the molecular dynamics of aqueous electrolyte solutions in biology, electrochemical systems, and nanofluidics.

Introduction

Aqueous electrolytes are important to life and a multitude of physical processes, some quite technological. Many electrolyte properties have been studied in detail.[1–7] However, there are still open questions about their dynamic structure, which is masked in the complex dielectric response of electrolytes to an external electric field. Figure 1a shows on a double-logarithmic scale the static electrical conductivity σ_{dc} of various aqueous electrolytes as a function of the solute concentration c. These are unambiguously divided into two groups. The conductivity of group A compounds (strong electrolytes) is directly proportional to the concentration, $\sigma_{dc} \sim c$, while the conductivity of group B compounds (weak electrolytes) is proportional to the square root of the concentration, $\sigma_{dc} \sim \sqrt{c}$. The direct comparison between the static electric properties of weak and strong electrolytes shows two important features. First, there is a clear gap between the two mentioned groups (for more data see Fig. S2 in the SI). Second, the curves depicting the scaled conductivity vs. the scaled concentrations of group A, and those of group B collapse into two uniform but different master curves (Figs. 1b and 1c). This behavior suggests a solute-independent conduction mechanism different for weak and strong electrolytes that the standard theory of electrolytic dissociation,[4] based on static data, does not track with the degrees of dissociation assumed from Arrhenius theory.

Here, using dielectric spectroscopy over an extended frequency range from 1 Hz to 20 GHz, the dynamic electrical properties of weak and strong electrolytes are studied and put in context to additional structural distinctions between these two types of electrolytes. To analyze and interpret the experimental data, a new model is hypothesized that can explain the observed features accounting for the interplay between solute and solvent via proton-exchange reactions, thus revealing the quantum nuclear effects previously missing in the models. The model supports the correlations in electrical conductivity of various electrolytes over a wide concentration range, and provides a physically agreeable explanation of the basic dielectric properties of aqueous electrolytes from the new viewpoint of the chemical dynamics between solute and solvent interactions.

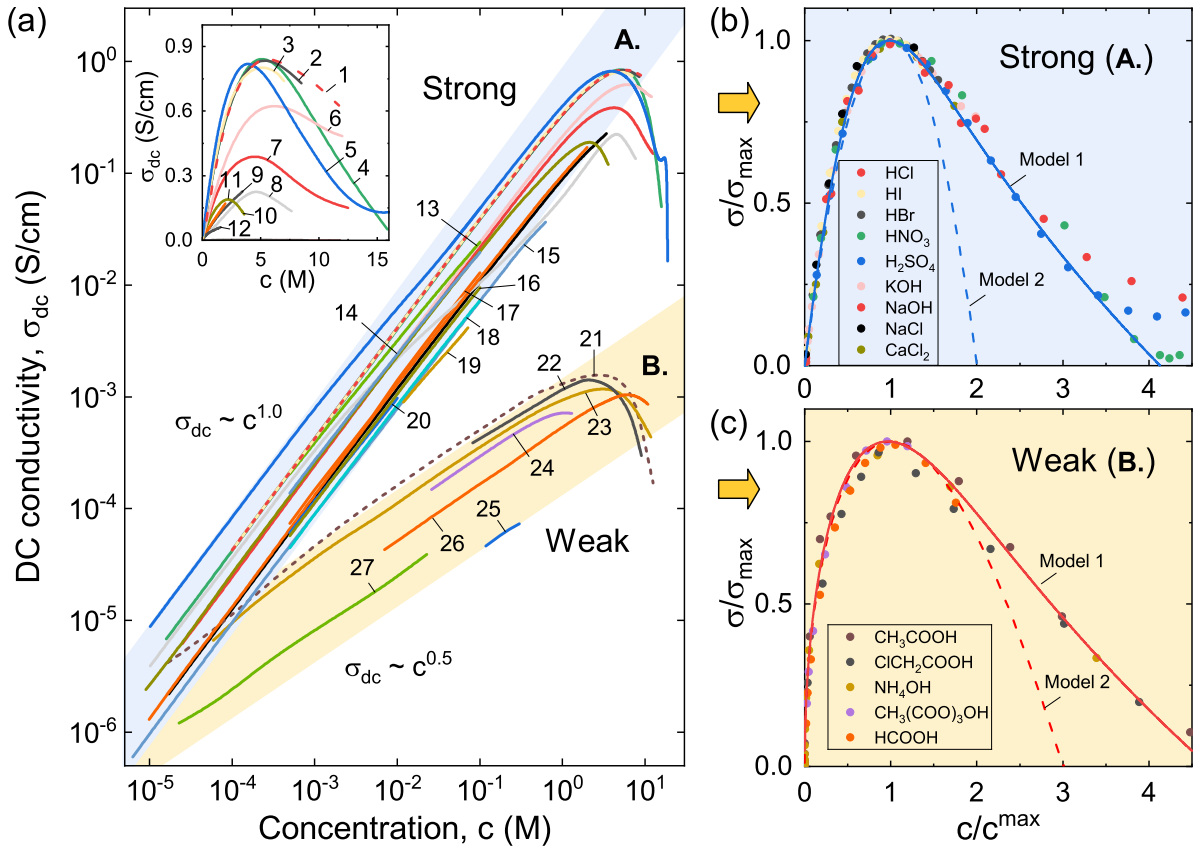

Figure 1: **Static electric properties of aqueous electrolyte solutions.** (**a**) The direct current conductivity, σ_{dc}, as a function of concentration c of various strong (from 1 to 20) and weak (from 21 to 27) electrolytes: 1 - HCl, 2 - HBr, 3 - HI, 4 - HNO_3, 5 - H_2SO_4, 6 - KOH, 7 - NaOH, 8 - H_3PO_4, 9 - NaCl, 10 - $CaCl_2$, 11 - KNO_3, 12 - SO_2, 13 - $AlCl_3$, 14 - $BaCl_2$, 15 - $CuSO_4$, 16 - LiCl, 17 - NH_4Cl, 18 - CH_3COONa, 19 - $NaHCO_3$, 20 - KH_2PO_4 , 21 - CH_3COOH, 22 - $ClCH_2COOH$, 23 - NH_4OH, 24 - $CH_3(COO)_3OH$, 25 - H_2S, 26 - HCOOH, 27 - H_2CO_3.[2,8,9] The graph in double-logarithmic scale demonstrates the splitting of the curves into two distinct groups with linear (group A, strong electrolytes) or square-root (group B, weak electrolytes) dependencies of σ_{dc} on c. The inset shows the same data in the commonly used linear scales. (**b**) and (**c**) Concentration dependencies of electrolyte solutions (see legends) normalized to the maximum of $\sigma_{dc}(c)$ (see Table S2 in SI for coefficients). The dependencies collapse into a single master curve, different for strong and weak electrolytes. The continuous and dashed red and blue curves are calculated with the models 1 and 2 (see the main text and the SI). The colored areas are guides for the eyes.

Results and Discussion

Experimental

Commercial impedance analyzers were used to study the response of aqueous electrolytes to an external electric field of variable frequency (see Methods). Using the solutions' complex impedance measurement data, we determined the frequency-dependent dielectric function $\epsilon^*(\nu)$ variations with the solute concentration c from 10^{-7} to 10^{1} mol/l in the 275-to-333 K temperature range. The studied spectral range covers the molecular dynamics from 1 ms down to 0.1 ns thus accounting for the intermolecular motion as well as the interaction of solute and solvent. Unlike previous studies,[2,7,10–15] experiments were performed over a large frequency range and a comparative point-by-point analysis of the weak and strong electrolytes was carried out. This allowed the distinction of correlations between the weak and strong electrolytes which have not been quantified heretofore. To understand the dielectric response of electrolytes, a mechanism is suggested that describes the experimental curves, avoiding contradictions such as negative hydration[16] or an ionic mobility larger for weak electrolytes than for strong electrolytes at high dilution.[4] Further, the proposed model is in good agreement with results obtained by other methods.[17–19]

Figure 2 shows the broadband dielectric spectra of both weak and the strong aqueous electrolytes, acetic acid (left) and hydrochloric acid (right), respectively. The upper and the middle panels represent the real ϵ' and the imaginary ϵ'' parts of the dielectric constant, respectively; the lower panels represent the dynamic conductivity $\sigma = \epsilon''\epsilon_0\omega$. The dots are experimental data. The colored curves represent the conjugate of a single Debye function[20] and the static conductivity: $\epsilon^* = \epsilon_\infty + i\sigma_{dc}/\epsilon_0\omega + (\epsilon_s - \epsilon_\infty)/(1 + i\omega\tau)$, where $\omega = 2\pi\nu$ is the angular frequency, ϵ_0 is the vacuum permittivity, σ_{dc} and ϵ_s are the static conductivity and the static dielectric constant, respectively, ϵ_∞ is the dielectric constant at high frequencies, and τ is the relaxation time. The fit parameters are given in Table S1 (see SI). The function satisfactorily describes the experimental data over a large frequency range except for the

high-frequency part of the spectra of the weak electrolyte (this particular point is explained further below). The spectrum at concentration c=0 is for pure water, which is shown in grey and serves as a common reference spectrum for both types of electrolytes.

As the concentration of the solute increases, the dielectric response of water changes as indicated with the yellow arrows (Fig. 2). The direct comparison of the spectra of the weak and strong electrolytes shows that some parameters such as the static dielectric constant, ϵ_s, and the high-frequency microwave conductivity, σ_{ac}, change concomitantly (Fig.3, a and b), while the curves of the dielectric relaxation times $\tau_D = \nu_r^{-1}$, where ν_r is the relaxation frequency (see the maximum in Fig. 2, middle panels), diverge (Fig.3c). An increase in c causes a decrease in ϵ_s or, in other words, a polarization suppression (Fig. 3a). Apart from the prediction of the electrolytic dissociation model that a weak electrolyte dissociates at low concentration, causing a larger depolarization (Fig. 3a, dashed line), the solute suppresses the dielectric constant proportionally to the concentration over the entire range. Note that the weak electrolyte has a lower polarization suppression efficiency as it requires a ten-times larger molarity to reduce ϵ_s of water to the same value as that for a strong electrolyte (as explained further below).

The suppression of σ_{ac} (Fig. 3b) is proportional to the concentration c over the entire range except for highly concentrated solutions, for which σ_{ac} starts diverging for both weak and strong electrolytes. The dielectric relaxation time τ_D follows the same trend shown in Fig. 3c. Note that the dielectric relaxation band of a strong electrolyte (Fig.2, middle panel) consists of one relaxation mode, while the response of a weak electrolyte contains two superimposed relaxation bands (Fig. S3 in SI). The first mode is presumably an intrinsic water band, and the second mode is a band of dissolved solute clusters, similar to that observed for emulsions.[21] The temperature dependence of the conductivity plateaus, σ_{dc} and σ_{ac} (Fig. 2, bottom panels), demonstrates that there is a single activation energy for each plateau. For strong electrolytes, the activation energy, $E_a = 0.09 \pm 0.02$ eV, coincides for both plateaus (Fig. S7 in SI). Similar values of E_a were observed for other strong electrolytes[12]

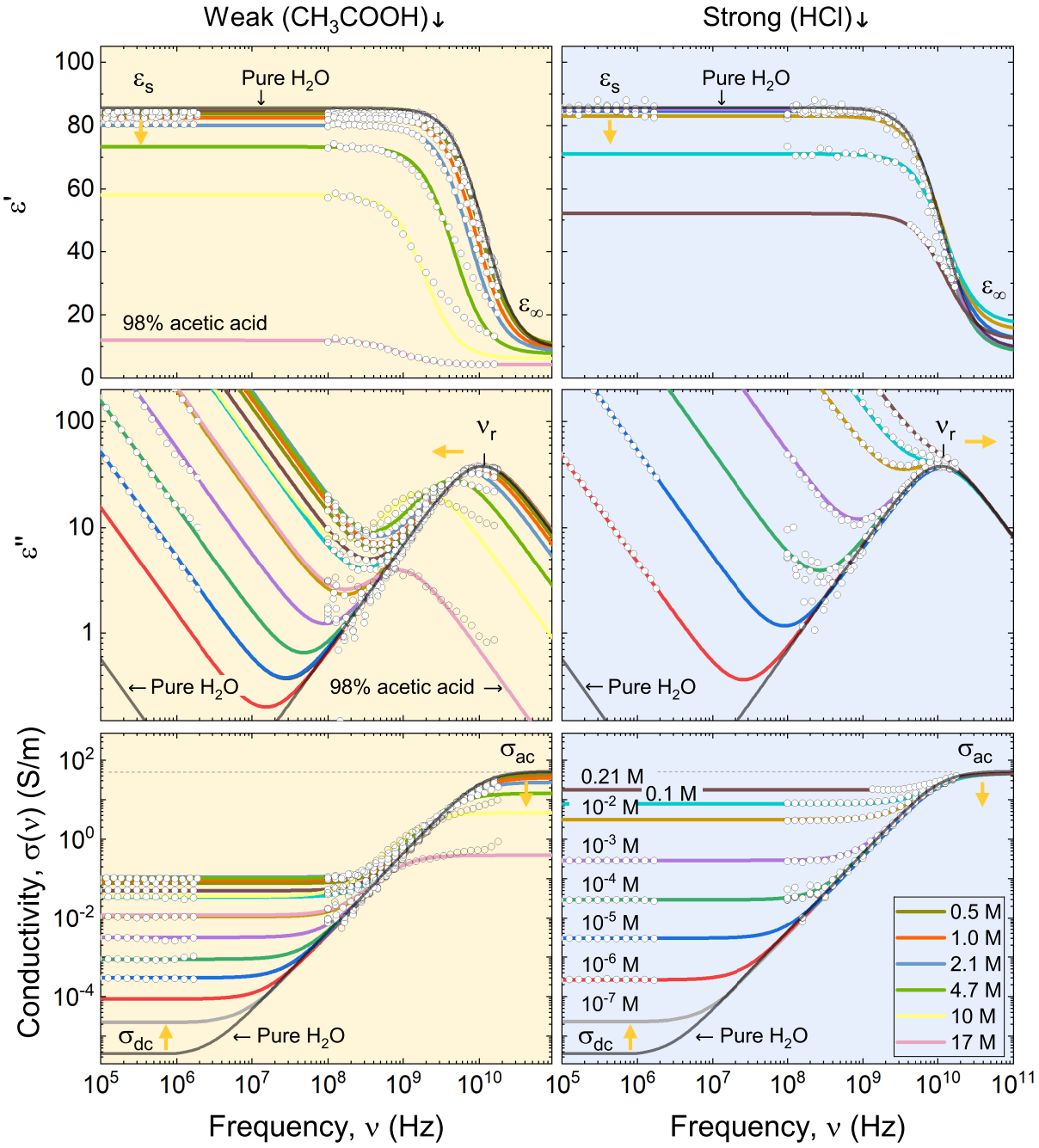

Figure 2: **Dynamic electric properties of aqueous electrolyte solutions.** The dielectric response of solutions of acetic acid (weak electrolyte, left-hand side) and hydrochloric acid (strong electrolyte, right-hand side). The top and the middle panels are the real, ϵ', and the imaginary, ϵ'', parts of the dielectric constant, and bottom panels are the dynamic conductivity, σ. The open symbols are experimental data, colored curves are the conjugate of the Debye relaxation, and the DC conductivity (see Table S1 in SI for parameters). The grey curves are for pure water (c=0). The numbers near the curves are concentrations (M $\equiv$ mol/l). The yellow arrows indicate the direction of the spectral parameters change with the increase of the concentration c. For further details see Fig. 3.

assuming the same conduction mechanism for all strong electrolytes, regardless of the nature of the solute. For the acetic acid, in contrast, the activation energies are concentration-dependent with $E_a = 0.12 \pm 0.02$ eV for σ_{ac} and $E_a = 0.14 \pm 0.02$ eV for σ_{dc} (Fig. S7 in SI). Hence, in addition to the gap between the groups A and B (Fig. 1a), and the diverging relaxation time (Fig. 2c), weak and strong electrolytes also differ in the DC conductivity mechanism. These three differences between weak and strong electrolytes are beyond the scope of the theory of electrolytic dissociation[4] and will be addressed using an improved model that includes the dynamic conductivity.

The mechanism of dynamic conductivity

A unified mechanism of dynamic conductivity of pure water from direct current to terahertz was recently proposed.[23,24] In short, two plateaus of conductivity, σ_{dc} and σ_{ac}, (Fig. 2) are considered to be associated with the dynamics of excess protons (H_3O^+) and proton holes (OH^-), whose mobility depends on the time scale of observation or the measurement frequency. The ions are formed by spontaneous tunneling of protons between water molecules with the formation of ionic species (Fig. 3d, red dots) among neutral water molecules (open circles). Although ions are short-lived, their concentration is large $c_0 \approx 1$ mol/l.[25] So, the plateau σ_{ac} of pure water (Fig. 2, bottom panels) corresponds to an in-cage dynamics of mutually screened ions, while σ_{dc} of pure water corresponds to the out-of-cage dynamics of the same ions.

Since the solute fosters the increase of σ_{dc} and suppresses σ_{ac} of pure water (Fig. 2, bottom panels, yellow arrows), the hypothesis is that the separation of the solute MX into ions M^+ and X^- (Fig. 3d, blue dots) is accompanied by their interaction with the short-lived intrinsic ions of water (Fig. 3d, red dots). The corresponding intermediate MOH and HX species are considered as the intrinsic ions of water neutralized by the solute. Such interactions simultaneously satisfy the decrease of the concentration of intrinsic ions of water, the suppression of the dielectric constant, ϵ_s, and the increase of ion mobility at low frequencies.

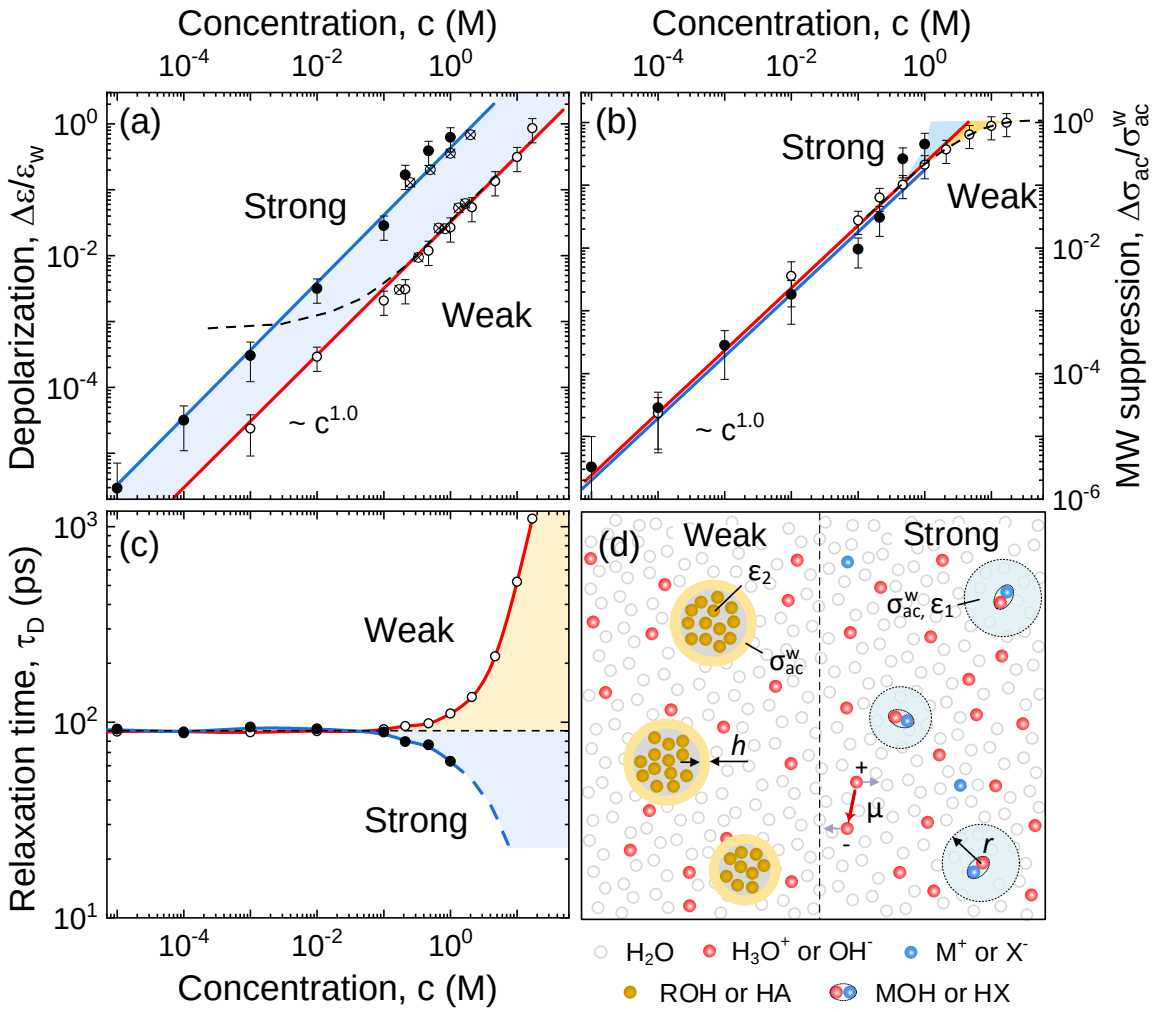

Figure 3: **Effect of solute on the dynamic properties of water and the corresponding microscopic model.** (**a**) The depression of the normalized dielectric constant (depolarization of water by the solute). (**b**) Suppression of the high-frequency conductivity σ_{ac} of water by the solute. (**c**) The shift of the relaxation time change of the relaxation time τ_D. Open and closed symbols are for CH_3COOH and HCl, respectively. The crossed circles show the literature data,[13,22] the red and the blue curves are fit, colored areas and dashed lines are guides for the eyes. (**d**) The model medium (structure), which corresponds to the dielectric data of weak (left) and strong (right) electrolytes. See the legend for the meaning of the symbols. The red arrow with μ is for the dipole moment of the H_3O^+-OH^- ionic pair.

The latter process occurs due to the breakdown of the relative screening potential of intrinsic water ions by their spontaneous neutralization by the ions of solute (Fig. 3d, blue areas). Note that Mendeleev argued that the nature of aqueous solutions assumes the formation of MOH or HX, rather than just M^+ and X^-,[26] but these ideas had not received much attention until recently when the quantum effect was shown to be important for the description of the properties of water and aqueous solutions.[24,27,28]

To support the scenario of neutralization of intrinsic ions of water by the ions of solute via proton exchange, note that the σ_{dc} of any strong electrolyte never exceeds $\sigma_{ac} \approx 1$ S/cm of pure water (Fig. 1, and Fig. 2, bottom panels, dashed line). As σ_{ac} is assigned to the full concentration of short-lived ions of water, c_0, the formation of any intermediate species of MOH and/or HX in aqueous solutions reduces c_0, and hence reduces σ_{ac} and ϵ_s accordingly (Fig. 3a and b). In parallel, the formation of intermediate species of MOH and HX causes a local perturbation of the electrostatic potential of intrinsic ions of water, thus, increasing the DC electrical conductivity, σ_{dc}, in proportion to the concentration c of the solute. This behavior is observed for all strong electrolytes (Fig. 1a) without exclusions. For the effective DC conductivity of a strong electrolyte solution, the model yields: $\sigma_{str}(c) = [\sigma_{ac}(2c_0 - c)c + \sigma_{dc}(c_0 - c)^2]/c_0^2$, where σ_{ac} and σ_{dc} are the high- and low-frequency conductivities of pure water, respectively. The formula satisfactorily fits the electrical conductivity of strong electrolytes over a wide range of concentrations (Fig. 1b, dashed blue curve, Model 2). The formula for the solid-blue curve is given by Eq. (3) in the SI. For both equations, it is assumed that the charge carriers in aqueous solutions are spontaneously-formed excess protons and proton holes, whose mobility is modulated by the species of solute. This assumption is a key component of the model, which differs from the classic electrolytic dissociation theory by Arrhenius.[29] The higher the concentration c is, the more excess protons have a large mobility via proton exchange reactions, thus, increasing the conductivity. Note that σ_{dc} of a solution reaches a maximum when the molar concentration c of the solute reaches the maximal concentration $c_0 = 1$ mol/l of intrinsic ions of water. The relationship between c_{max}

(Table S2 in the SI) and c_0 depends on the specific properties of the solution, such as the density, the molecular mass of the solute, and the solute-solvent dissociation-recombination rate, which we are not discussed here for simplicity.

The key experimental result of this study is the distinction between the spectra of weak and strong electrolytes over the entire frequency range, i.e. not restricted to the static conductivity limit. Notably, the spectra of weak electrolytes (Fig. 2) are similar to those observed for alcohol-water mixtures, aqueous emulsions, and colloidal solutions,[21,30,31] which are not homogeneous mixtures but two-phase systems. Moreover, the electrical conductivity of various nanocolloids shows the same square-root proportionality to concentration (Fig. S6 in SI) as observed for weak electrolytes (Fig. 1). Assuming by analogy that the molecules of a weak electrolyte interact stronger among each other than with water molecules, the formation of clustes of several molecules is considered, which are interpreted as "foreign" species present in the aqueous dielectric medium (Fig. 3d), and thus suggests a mechanism in which proton-exchange reactions between solute and solvent are similar to those described above for strong electrolytes, but which take place at the boundary of the islands only, within the layer of constant thickness, h (Fig. 3d, yellow rings). Thus, the electrolyte changes the conductivity within the shell around the island, and the solution has the effective electrical conductivity: $\sigma_{weak}(c) = [\sigma_{ac}(2c_0 - c)\sqrt{c} + \sigma_{dc}(c_0 - c)^2]/c_0^2$ that satisfactorily fits the experimental data for weak electrolytes (Fig. 1c, dashed red curve, Model 2).

According to this model, the electrodynamics of aqueous electrolyte solutions is determined by the proton tunneling between solute and solvent, i.e. nuclear quantum effects, the intensity of which depends on the boundary conditions, which are different for weak and strong electrolytes. The solute-irrelevant nature of these reactions explains a unified form of the conductivity dependencies for all strong (Fig. 1c) and all weak electrolytes (Fig. 1b). The sharply-defined distinction between groups A and B (Fig. 1) is due to different microscopic structures. In weak electrolytes, the species of the solute interact stronger with each other than with H_2O molecules, which leads to their clustering, while in the strong electrolytes

the species of solute and solvent are homogeneously mixed. In the first case, the solute-solvent reactions occur on the surface of the clusters, while in the second case they occur in the whole volume of the solution. This interpretation provides a physically transparent explanation of the difference between groups A and B in Fig. 1, which is characterized by a direct proportionality (group A) or the square-root proportionality (group B) of the electrical conductivity to the concentration c (see section 1 of the SI for details).

Model structures in Fig. 3d are different for weak and strong electrolytes, but both give an inverse proportionality of the effective dielectric constant to the concentration c. Indeed, the solute locally changes the dielectric constant of the water in the areas shown in grey and blue (Fig. 3d). The effective medium concept[32] for such a system gives: $\epsilon_{sol} = \epsilon_w$ - $c(\epsilon_w - \epsilon_{1,2})$, where ϵ_1 and ϵ_2 is the local dielectric constant of areas affected by the species of strong and weak electrolytes, respectively (Fig. 3d, blue and gray areas). This hypothesis is in good agreement with the experiment (Fig. 3a, colored lines). Thus, the structural schemes shown in Fig. 3d, fully explain the difference between the dielectric response of weak and strong electrolytes: the variation between the dielectric relaxation times (Fig. 3c), the gap between groups A and B (Fig. 1a) and the uniform dependence of the static electrical conductivity over the entire concentration range, while different for groups A and B (Fig. 1, b and c). Note that our model assumes the effects of spontaneous proton exchange between solute and solvent, which improves the theory of electrolytic dissociation and allows for better analysis and interpretation of the experimental data. For instance, X-ray absorption studies of the front of the edge of the K-edge electrons of the oxygen (O) atom in aqueous solutions depends on the concentration of cations (M^+), but not anions (X^-).[17] Indeed, only MOH molecules ($M^+ + OH^-$) contain an oxygen atom, while HX molecules ($H^+ + X^-$) do not because the latter reaction does not change the O-atom electronic structure. Thus, the absorption of X-rays studies indirectly support the data presented herein and the conclusions about solute-solvent interactions leading to the contention of quantum nuclear effects associated with electrolytic dissociation. Albeit, further experiments in this area are required to support

the proposed model and associated experimental data presented.

Conclusions

The static electric properties of the weak and strong electrolyte solutions clearly show distinct features the cause of which cannot be reduced to the variation of the degree of dissociation without additional assumptions. Here, the dynamic electric properties of weak and strong electrolytes were measured using broadband dielectric spectroscopy, which supports the idea of different solution structures. From our observations a new model is proposed that explains the experimental data for both the conductivity and the dielectric constant of aqueous solutions of electrolytes over the entire concentration range. The model explicitly accounts for the chemical reactions between solute and solvent or, in other words, for the nuclear quantum effects, which, although they have been discussed in recent years,[24,27,28] never were considered for the detailed analysis of the electrodynamic properties of aqueous electrolyte solutions. By accounting for the proton exchange between solute and solvent, a meaningful explanation of the electrodynamic data is provided in those concentration and frequency regions, which are not covered by the current models, including the series of Debye-Hückel approximations.[33] These results and model thus provide a more detailed picture of the mechanism underlying the electrodynamic properties of aqueous electrolytes, and may have profound implications in electrochemistry, biology, and neurosciences. For example, it provides impetus for the understanding of such phenomena as the change of the solubility of organic nonelectrolytes in the presence of salts,[34] the strong heterogeneous electric fields within the tissue in the extracellular space,[35] the increase of the electrostatic screening length in concentrated electrolytes,[36] and the formation of asymmetric excess proton hydration structures in acid solutions.[19]

Notably, this work provides new insights into the hundred-year-old dispute between Arrhenius and Mendeleev. Arrhenius insisted on the physical concept of electrolyte conduc-

tivity,[29] in which the species of solute MX dissociated into long-lived ions of M^+ and X^-, providing charge carriers for the electricity conduction. Mendeleev was not against the idea of splitting solute into ions, but he specifically noted the missing role of the solvent and the species of MOH and HX in the model.[26] In other words, he was aware of the role of chemical interactions between solute and solvent. As such the data presented herein offers new understanding of the dynamic structure of aqueous electrolytes and sheds interesting new light on this controversy, showing that both the ionic, M^+ and X^- and the molecular, MOH and HX, species contribute to the dielectric response of aqueous electrolyte solutions, though they may manifest themselves on different time scales, or from a spectroscopic viewpoint, over different frequency ranges.

Methods

Weak and strong electrolytes were prepared using commercially available concentrated solutions and deionized water. All solutions were made immediately before measurements to avoid the influence of atmospheric gases on their dielectric properties. The samples were tested by measuring their DC conductivity, which was found to be in good agreement with the known literature data. For dielectric measurements, we used two commercially available Keysight E4980A and N9917A dielectric analyzers. Low-frequency measurements in the range from 1 Hz to 20 MHz were performed in the parallel plate geometry using two round gold electrodes placed 3 mm apart. The samples were passed through the gap between the electrodes using a peristaltic pump with a controlled rotation speed. High-frequency spectra above 20 MHz were measured in the reflection mode using a coaxial cable with an open-end immersed in the sample. The dielectric constant $\epsilon^*(\omega)$ and the dynamic conductivity $\sigma(\omega)$ were calculated from the complex impedance using a standard procedure. All devices were calibrated before measurements and between each measurement. The spectra were recorded at four different temperatures in the temperature range from 5 to 60 ° C to obtain the ac-

tivation energies of the conduction plateaus. The sample temperature was controlled by a Peltier element with an accuracy better than 0.2 ° C.

Acknowledgement

We thank Prof. Anton Andreev and Dr. Viktoria Nikitina for fruitful discussions, Dr. Pavel Kapralov for technical support, and Mr. Matheus Pinheiro for his interest and curiosity during the internship at Skoltech in 2020.

Author contributions statement

A.R. and V.G.A. conceived the experiments and conducted the measurements, A.R., V.G.A., and H.O. analyzed the results and proposed the models, V.G.A. wrote the manuscript, H.O. and K.S. supervised the project and revised the manuscript. All authors contributed to the research.

Supporting Information Available

1. On the electrical conductivity of an effective dielectric medium; 2. Additional data on the electrodynamic properties of aqueous solutions: Fig. S1 to S7; Tab. S1 to S3; Ref. [1-7].

References

(1) Bockris, J. O.; Reddy, A. *Modern Electrochemistry*; Plenum: New York, 1970.

(2) Hasted, J. *Aqueous Dielectrics*; Chapman and Hall: London, 1973.

(3) Shock, E. L.; Oelkers, E. H.; Johnson, J. W.; Sverjensky, D. A.; Helgeson, H. C. Calculation of the thermodynamic properties of aqueous species at high pressures and

temperatures. Effective electrostatic radii, dissociation constants and standard partial molal properties to 1000 ° C and 5 kbar. *J. Chem. Soc., Faraday Trans.* **1992**, *88*, 803–826.

(4) Wright, M. R. *An Introduction to Aqueous Electrolyte Solutions*; Wiley: New York, 2007.

(5) Marcus, Y. *Ions in Water and Biophysical Implications: From Chaos to Cosmos*; Springer: Berlin, 2015.

(6) Bagotsky, V. S.; Skundin, A. M.; Volfkovich, Y. M. *Electrochemical Power Sources: Batteries, Fuel Cells, and Supercapacitors*; Wiley: New Jersey, 2015.

(7) Balos, V.; Imoto, S.; Netz, R. R.; Bonn, M.; Bonthuis, D. J.; Nagata, Y.; Hunger, J. Macroscopic conductivity of aqueous electrolyte solutions scales with ultrafast microscopic ion motions. *Nature Comm.* **2020**, *11*, 1611–8.

(8) Lide, D. *CRC Handbook of Chemistry and Physics, 101st Edition*; Taylor & Francis: Boca Raton, 2020.

(9) Kohlrausch, F.; Holborn, L. *Das Leitvermögen der Elektrolyte*; Teubner: Leipzig, 1916.

(10) Buchner, R.; Hefter, G. Interactions and dynamics in electrolyte solutions by dielectric spectroscopy. *Phys. Chem. Chem. Phys.* **2009**, *11*, 8984–8999.

(11) Yada, H.; Nagai, M.; Tanaka, K. The intermolecular stretching vibration mode in water isotopes investigated with broadband terahertz time-domain spectroscopy. *Chem. Phys. Lett.* **2009**, *473*, 279–283.

(12) Gulich, R.; Köhler, M.; Lunkenheimer, P.; Loidl, A. Dielectric spectroscopy on aqueous electrolytic solutions. *Radiation and Environmental Biophysics* **2009**, *48*, 107–114.

(13) Lyashchenko, A.; Lileev, A. Dielectric Relaxation of Water in Hydration Shells of Ions. *J. Chem. Eng. Data* **2010**, *55*, 2008–2016.

(14) Shcherbakov, V. V.; Artemkina, Y. M.; N., K. E. Dielectric properties and high-frequency conductivity of the sodium chloride-water system. *Russ. J. Inorg. Chem.* **2014**, *59*, 922–926.

(15) Cota, R.; Ottosson, N.; Bakker, H. J.; Woutersen, S. Evidence for Reduced Hydrogen-Bond Cooperativity in Ionic Solvation Shells from Isotope-Dependent Dielectric Relaxation. *Phys. Rev. Lett.* **2018**, *120*, 216001.

(16) Buchner, R.; Samani, F.; May, P. M.; Sturm, P.; Hefter, G. Hydration and Ion Pairing in Aqueous Sodium Oxalate Solutions. *Chem. Phys. Chem.* **2003**, *4*, 373–378.

(17) Nagasaka, M.; Yuzawa, H.; Kosugi, N. Interaction between Water and Alkali Metal Ions and Its Temperature Dependence Revealed by Oxygen K-Edge X-ray Absorption Spectroscopy. *J. Phys. Chem. B* **2017**, *121*, 10957–10964.

(18) Rizzuto, A.; Cheng, E.; Lam, R.; Saykally, R. Surprising Effects of Hydrochloric Acid on the Water Evaporation Coefficient Observed by Raman Thermometry. *J. Phys. Chem. C* **2017**, *121*, 4420–4425.

(19) Fournier, J.; Carpenter, W.; N.H.C., L.; A., T. Broadband 2D IR spectroscopy reveals dominant asymmetric $H_5O_2^+$ proton hydration structures in acid solutions. *Nature Chem.* **2018**, *10*, pages932–937.

(20) Debye, P. *Polar Molecules*; Chemical Catalog Co.: New York, 1929.

(21) Skodvin, T.; Sjöblom, J.; Saeten, J. O.; Urdahl, O.; Gestblom, B. Water-in-Crude Oil Emulsions from the Norwegian Continental Shelf. *J. Colloid. Interf. Sci.* **1994**, *166*, 43–50.

(22) Bohigas, X.; Tejada, J. Dielectric properties of acetic acid and vinegar in the microwave frequencies range 1–20 GHz. *J. Food Eng.* **2009**, *94*, 46–50.

(23) Artemov, V. A unified mechanism for ice and water electrical conductivity from direct current to terahertz. *Phys. Chem. Chem. Phys.* **2019**, *21*, 8067–8072.

(24) Artemov, V. G. *The Electrodynamics of Water and Ice*; Springer: Cham, Switzerland, 2021.

(25) Artemov, V. G.; Uykur, E.; Roh, S.; Pronin, A. V.; Ouerdane, H.; Dressel, M. Revealing excess protons in the infrared spectrum of liquid water. *Sci. Rep.* **2020**, *10*, 11320.

(26) Mendeleev, D. I. Note on dissociation of solutes [in Russian]. *J. Russ. Phys. Chem. Soc.* **1889**, *21*, 213–217.

(27) Ceriotti, M.; Fang, W.; Kusalik, P. G.; McKenzie, R. H.; Michaelides, A.; Morales, M. A.; Markland, T. E. Nuclear Quantum Effects in Water and Aqueous Systems: Experiment, Theory, and Current Challenges. *Chem. Rev.* **2016**, *116*, 7529–7550.

(28) Roy, S.; Schenter, G. K.; Napoli, J. A.; Baer, M. D.; Markland, T. E.; Mundy, C. J. Resolving Heterogeneous Dynamics of Excess Protons in Aqueous Solution with Rate Theory. *J. Phys. Chem. B* **2020**, *124*, 5665–5675.

(29) Arrhenius, S. Hydration versus Electrolytic dissociation. *Phil. Mag.* **1889**, *28*, 30–38.

(30) Brai, M.; Kaatze, U. Ultrasonic and hypersonic relaxations of monohydric alcohol/water mixtures. *J. Phys. Chem.* **1992**, *96*, 8946–8955.

(31) Grosse, C.; Tirado, M.; Pieper, W.; Pottel, R. Broad Frequency Range Study of the Dielectric Properties of Suspensions of Colloidal Polystyrene Particles in Aqueous Electrolyte Solutions. *J. Colloid. Interf. Sci.* **1998**, *205*, 26–41.

(32) Choy, T. *Effective Medium Theory*; Clarendon Press: Oxford, 1999.

(33) Landau, L.; Lifshitz, E. *Physical Kinetics: Course of Theoretical Physica - Volume 10*; Pergamon Press: New York, 1981.

(34) Gibb, B. Hofmeister's curse. *Nature Chemistry* **2019**, *11*, 963–965.

(35) Savtchenko, L.; Poo, M.; Rusakov, D. Electrodiffusion phenomena in neuroscience: a neglected companion. *Nature Reviews Neuroscience* **2017**, *18*, 598–612.

(36) Smith, A. M.; Lee, A. A.; Perkin, S. The Electrostatic Screening Length in Concentrated Electrolytes Increases with Concentration. *J. Phys. Chem. Lett* **2016**, *7*, 2157–2163.